Diyala Journal of Engineering Sciences

Journal homepage: https://djes.info/index.php/djes

ISSN: 1999-8716 (Print); 2616-6909 (Online)

Effect of Adding Heat Exchanger on the Refrigeration System Performance

Maytham Neamah Jasim*, Yaser Alaiwi

Department of Mechanical Engineering, Altinbaş University, Istanbul 34217, Turkey

ARTICLE INFO

Article history:
Received November 12, 2022
Revised April 7, 2023
Accepted April 10, 2023
Available online April 15, 2023

Keywords:
Shell and tube
Coefficient of performance (COP)
Engineering Equation Solver (EES)
Condenser
Subcooling

ABSTRACT

Internal or liquid-suction heat exchangers are used with the main goal of ensuring the entry of refrigerant in the liquid phase to the expansion device. The greatest COP gain is primarily determined by the thermodynamic parameters linked to the relative increase in refrigerating effect. Large latent heat of vaporisation refrigerants often does not gain as much from condenser subcooling in support of a cooling system. Computational fluid dynamics (CFD) is used to study the effects of the turbulence model, which requires the solution of two transport equations. A technique was developed to study the thermal effect on the heat exchange process between two fluids. To observe the temperature effect on 17 tubes, the diameter was altered twice, first to 6 mm and then to 4 mm. The flow procedure transpired in one direction, and the tube housing the tubes had a diameter of 50 mm. In the best-case scenario, the pipe diameter is 4 mm, and the heat exchanger is 300 mm in length. The results indicate an improved enthalpy of 423.2 h [KJ/M] in the simulated cases. The length of the heat exchanger greatly affects the values of the exit temperatures and the temperature difference. For a length of 225 mm, the temperature reached 15.73 °C, and for 300 mm, it reached 13.847 °C. The significant reduction in temperatures increases the coefficient in the refrigeration cycle. A high coefficient of cooling in the heat exchanger appears when the length is 300 mm compared with other lengths.

1. Introduction

An in-depth analysis of the thermal and flow characteristics of the inner heat exchanger for R1234yf and R134a refrigerants was conducted. This analysis explored the correlation between the coefficient of performance (COP) and the overall heat transfer coefficient under operational conditions. In addition, the effects on the heat exchanger's length and efficiency, annular space and strain drop were examined. The huge annular area of the internal heat exchangers often results in unfavourable intensity movement coefficients because laminar streams through the annular region are unsuitable for increasing COP [1].

LSHX and R290 have enormous financial potential as a replacement for current systems in the future due to their low potential for unnatural weather change and nearly identical refrigerant characteristics to those of R22, R410A, R290 and R32. Subcooling was examined by a fluid pull heat exchanger (LSHX) on the display of a cooling framework using these refrigerants. [2]. The temperature at the condenser outlet decreased by 2.2 °C as a result of the reduced blower release pressure. The cooling capability of the split-type climate control system is 2.5 kW [3].

* Corresponding author.
E-mail address: neamahmaytham@gmail.com
DOI: 10.24237/djes.2023.16201

The majority of coolers uses a fume pressure cycle (VCC), which considers their other available possibilities. Three classes were considered, namely, multi-stage cycles, development misfortune recovery cycles and double evaporator cycles. The private coolers use non-VCC advancements including thermoelastic, thermoelectric, attractive and thermoacoustic technologies. [4]. The IHX's maximum amount of entropy was considered while recreating the framework. For R152a and R134a, the maximum entropy age occurs at 66 percent viability. The framework was determined to operate at its best practicable level when the R1234ZE refrigerant was used. For each occurrence, the effects of subcooling and superheating are assessed. [5].

The internal regenerative heat exchange mechanism of a closed-loop cooling system recovers important cooling and heating energy. The best recovery techniques include regenerative heat exchangers, which are comparable to the pull-line heat exchanger in fume pressure frameworks. Each of the three recovery techniques is shown with its actual implementation, a review of its continuing level of development and appraisals of its benefits, drawbacks and distinguishing characteristics. [6]. The findings demonstrated that the hot stream was primarily impacted by the transient shift caused by the supercritical operating conditions. The shift in mass stream rate causes a decrease in the intensity move rate and warm viability at the start of the framework's activity. The transient behaviour of the presentation coefficient has a backward connection with the warm sufficiency of the inner heat exchanger. [7]. The cooling limit of R1234ze (E) is expanded to the same extent as R134a by using an open-type blower that is 43 percent larger and an interior heat exchanger that is 25 percent more efficient. R450A is essentially started using IHX. Unadulterated hydrofluoroolefins (HFOs), unsaturated organic molecules made of carbon, fluorine and hydrogen were recommended as replacement for this liquid. Nonetheless, framework adjustments are often anticipated to achieve appropriate execution [8]. R1234yf is used as a drop-in replacement for R134a in the experimental study for three household refrigerators that are identical to those in this work. Compared with R134a, this approach leads to a slight increase in energy consumption of 4%. TEWI research finally revealed that this value was 1.07 percent higher than that of R-134a. [9]. In steady state settings with subcooling temperatures, evaporators with R290 or R600a may achieve −30 °C. R404a and R22 achieved lower values at −24 °C and −22 °C, respectively. R290 and R600a, combined 50/50, have qualities that are comparable to those of R404A and might be used as a replacement. The RCI increases by 3.91 percent, 7.78 percent and 11.87 percent [10]. The R1234yf framework has a 4.0%–7.0% lower cooling limit and a 3.6%–4.5% COP. For a blower speed of 800–1800 rpm, the COP is 0.3–2.9 percent lower than that of the R134a framework. With and without the IHX, the second regulation effectiveness of R12 34 YF was expanded by 1.5%–4%. At all blower speeds, the energy destruction ratio (EDR) of the framework was 0.5%–3.3% [11]. Only low-GWP refrigerants are allowed in wealthy nations in the medium future. One of the most promising among them is R1234ze. The majority of HVACR applications may employ this refrigerant because of its strong environmental attributes. When combined with other refrigerants, the final GWP value is also significantly reduced [12]. As condenser subcooling increases, the trade-off between growing refrigerating effect and specific pressure work causes the COP to reach an extreme condition.

The extent of the potential increase in COP is still uncertain because of the thermodynamic limits associated with the general expansion in refrigerating effect, i.e., fluid explicit intensity and idle intensity of vaporisation [13]. An overview of several improvements and enhancement techniques for a fume pressure refrigeration cycle-based vehicle temperature control system is provided in this article. This essay primarily consists of two sections. The first section includes a study on achieving improved auto cooling (AAC) framework's mandatory and optional components. The second section assesses the functional

administration and control of energy to operate the AAC system [14].

The study's objective is to use refrigeration cycles to implement heat recovery concepts in HVAC applications. It focuses on how energy recovery relates to the areas of heating, ventilation and air conditioning. The condenser's lost energy is used to heat or pre-heat household water. Thermal modelling for the entire system is produced, and a corresponding iterative code is shown. The outputs of calculations that use the code offer magnitude orders for energy management and savings [15]. The R1234YF mobile air conditioning (MAC) system's potential for performance improvement was investigated using thermodynamic cycle analysis. We considered the effects of compressor coefficient, subcooling at the condenser outlet and superheat at the evaporator outlet. The results showed that the benefits of superheat for cooling capacity and system coefficient of performance were negligible (COP). The compressor's isentropic coefficient had a substantial role in the increase in system COP. The compressor coefficient should be increased, and an internal heat exchanger should be installed; these approaches are the best for MAC system modification [16].

Erosion coefficients for nano-oil with a convergence of 1–3 g/L are 12.9%–19.6% lower than for pure mineral oil. Testing has been conducted to determine the duration for which nanoparticles can remain suspended in mineral oil under fixed conditions. The grating coefficients of the nano-oil dramatically decrease as the nanoparticles in the mineral oil increases, particularly at relatively low applied loads [17]. The household and commercial buildings often use split-type air conditioners (A/Cs). To save considerable energy, the appearance of this A/C might be enhanced. An ejector might be used in conjunction with temperature control systems to increase COP. The mathematical results showed that, individually, spout and blending chamber diameters of 1.1- and 2.5-mm result in the perfect COP improvement. Separate increases in COP of 4.17, 11.14 and 13.78 percent have been observed for the modified ejector cycle at surrounding temperatures of 30 °C, 35 °C and 40 °C, respectively [18].

The energy coefficient and relative CO2 emissions of two R134a drop-in replacements with low global warming potential (COP) were studied. Three characteristics were considered: COP, cooling capacity and volumetric coefficient. Various evaporation and condensation temperature values were mixed during tests in a vapor compression system under observation. The COP fluctuations between the two replacements are minimised using an internal heat exchanger [19]. A numerical method has been suggested for determining the motive nozzle and constant-area of an ejector used as an expansion device. Capillary tubes are often used when installing split-type air conditioners in locations with moderate to high outside air temperatures. The results demonstrated that despite temperature changes, the ejector's diameter (1.14 mm) remained consistent [20].

In this work, supercritical CO2 microtube heat exchangers composed of the superalloy Haynes 282 are optimised using a 2D numerical shell-and-tube heat exchanger performance prediction model. These heat exchangers are improved via particle swarm optimisation, producing small and affordable designs with power densities of approximately 20 kW/kg and costs per conductance of approximately $5 K/W [21].

In this work, shell and tube heat exchangers with round and hexagonal tubes operating in parallel and counter-flow configurations at different flow velocities were investigated experimentally. The heat transfer rate, temperature drop and heat transfer coefficient were calculated using three turbulence models (SST). When CFD is used for counter and parallel flow, the rate of heat transfer is related to fluid velocities and the number of tubes turns. The flow in hexagonal tubes may be disturbed more readily than in round tubes, thereby increasing the rate of heat transfer [22], exhibiting cooling capacity and heat rejection. Nevertheless, the research objectives are limited to determining the coefficient of cooling by adding heat exchangers with variable designs.

2. Methodology

To achieve accurate results, two programs should be combined given that the ANSYS program was used to study the heat exchanger and its heat transfer method, contributing to a comprehensive understanding of the obtained results. The EES works by drawing a cycle diagram for the refrigeration system and showing the properties.

2.1 General Mass, Energy and Exergy Equations of EES

The conservation of mass equation for the system is expressed as follows [23]:

$$\sum \dot{m}_{in} = \sum \dot{m}_{out}, \quad (1)$$

where $\sum \dot{m}_{in}$ is the total mass flow entering the system per unit time, and $\sum \dot{m}_{out}$ is the total mass flow exiting the system per unit time.

The energy balance for each component is based on the first law of thermodynamics for the system [23], which is expressed as follows:

$$\dot{Q} + \dot{W} = \sum \dot{m}_{out} h_{out} - \sum \dot{m}_{in} h_{\text{in}}, \quad (2)$$

where $\dot{Q}$ is the heat transfer per unit time, $\dot{W}$ indicates the work performed by the control volume per unit time, and h_{in} is the specific enthalpy per mass, entering the system. Moreover, h_{out} refers to specific enthalpy per mass. leaving the system.

Different from mass and energy, entropy is not conserved in open and closed systems because it is produced by irreversibility. In open systems, the entropy balance can be expressed as follows:

$$\dot{E} = \dot{m}\psi \quad (3)$$

$$\text{COPcooling} = \frac{T_{\text{COLD}}}{T_{\text{HOT}} - T_{\text{COLD}}} \quad (4)$$

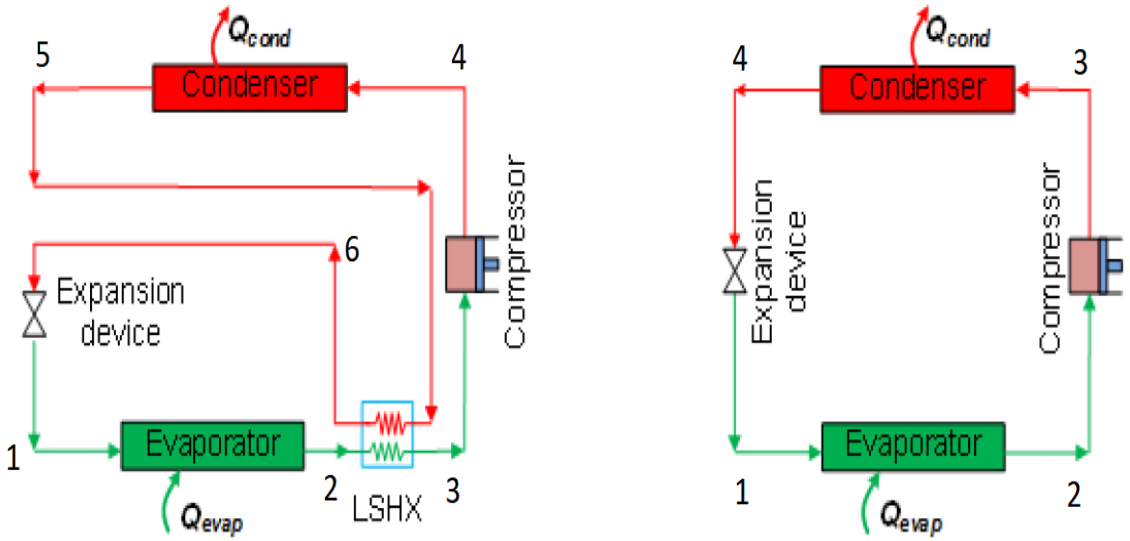

Figure 1. Schematic diagrams of a vapor compression refrigeration cycle. (a) Cycle with LSHX (b) Basic cycle.

2.2 Computational analysis using ANSYS package

Studies in computational fluid dynamics (CFD) are conducted to obtain considerable knowledge about the flow. A model of k-e is used to highlight the impact of the turbulence model by solving a two-transport equation. Therefore, these cartesian coordinate systems may be solved using numerical solution methods (x, y and z). The geometry in three dimensions is produced.

ANSYS version 19 is implemented here to generate and grip the system geometry and run the simulations.

2.2.1 Assumptions

In the current study, R140A is considered the running liquid, and the characteristics of flow are assumed to be:

- steady flow, 3D,
- Newtonian,
- incompressible, and
- turbulent.

2.2.2 Governing equations

The governing equations to be solved include the continuity, momentum and the equation of the energy.

- Mass conservation (continuity) [23]

  Mass conservation is expressed mathematically as the continuity equation, which relates the rate of mass flow into and out of a control volume to the change in mass within the volume. The continuity equation is derived from the principle of conservation of mass, and expressed as follows:

$$\nabla \cdot (V) = 0. \tag{5}$$

- Momentum Equation [23]

$$\nabla \cdot (\rho \dot{V} \dot{V}) = -\nabla p + \nabla \cdot (\bar{\tau}) \tag{6}$$

The stress tenser $\bar{\tau}$ is given by the following [23]:

$$\bar{\tau} = \mu \left[\left(\nabla \vec{V} + \nabla \vec{V}^T \right) - \frac{2}{3} \nabla \cdot \vec{V} I \right] \tag{7}$$

- Energy Equation [23]

$$\nabla \cdot (\dot{V}(\rho E)) = \nabla (k \nabla T - \rho C \dot{V} T') \tag{8}$$

- Turbulence Equations

To account for the existence of robust matter, sinks have been included into all of the disturbance situations in the mellow and stable regions. Similar to the force sink word, the sink phrase has the following form:

$$S = \frac{(1-\beta)^2}{(\beta^2+\varepsilon)} A_{mush} \varphi, \tag{9}$$

where φ is the mushy zone constant $(k, \varepsilon \text{ and } \omega)$ and represents the turbulence quantity being addressed A_{muss}.

2.2.3 System geometry

The system architecture shown in Figure 2 consists of a shell and tube type heat exchanger with variable lengths to identify the thermal effect in the heat exchange process between the two fluids. Three different lengths were considered: 150, 225 and 300 mm. The diameter of the tubes was changed twice, once to 6 mm and once to 4 mm, to determine the thermal effect and the number of tubes (17). Moreover, the tube containing the small tubes has a diameter of 50 mm, and the flow process occurred in the opposite direction.

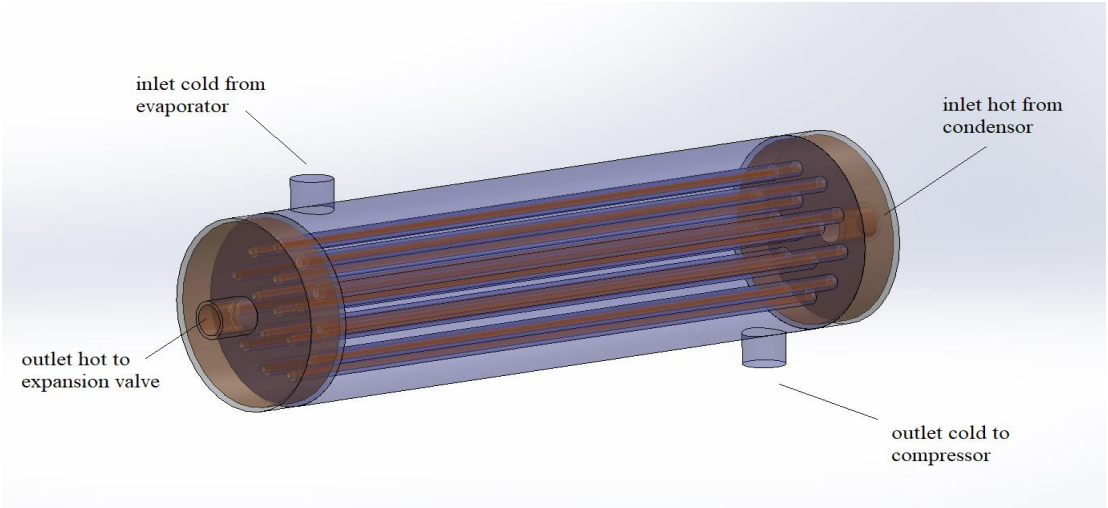

Figure 2. Geometry shape

2.2.4 *Mesh generation*

Unstructured grids tend to work effectively for complicated geometries; thus, a tetrahedron grid was used in this investigation. In ANSYS, users should provide input in a single phase to generate a mesh for a solid geometry or a 3D model. In this work, a total of 8,383,882 cells were collected, as shown in Fig. 3.

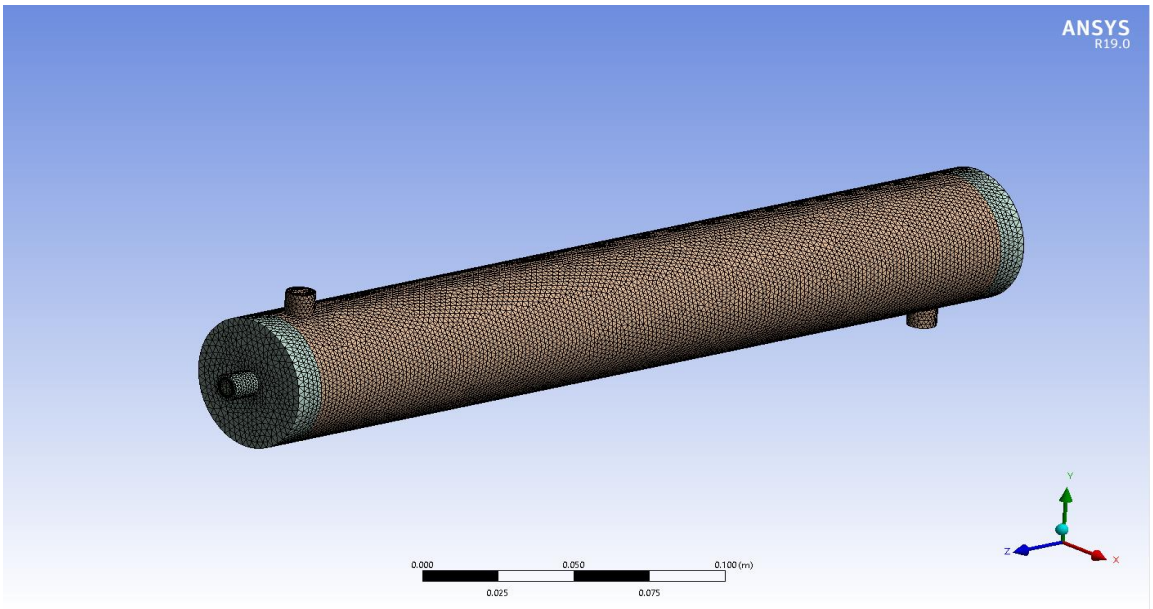

Figure 3. Mesh generated

Table 1: Mesh independency

Case	Number of elements	Max. temperature (°C)
1	2742012	55.253
2	4624300	53.911
3	6457344	53.871
4	8383882	53.863

2.2.5 *Conditions of the boundary*

The pressures and temperatures extracted from the EES program (Table 2) were entered as the results of the CFD program, which is considered a boundary condition. The EES program finds cycle variables in the form of exact equations based on the ASHRAE source. The required capacity of the compressor is 10,033 Btu/hr (0.83 tons).

Table 2: Boundary conditions of EES

point	P [bar]	T [C]
1	678.3	−5.081
2	678.3	−5
3	932.5	4.975
4	1889	52.89
5	1889	30
6	1531	22.06

2.2.6 *Initial conditions*

The flow field cannot be determined until after iteration has begun, a best estimate is required prior to any progress towards a solution. All parameters in this study are set relative to the inlet boundary conditions of the inner pipe.

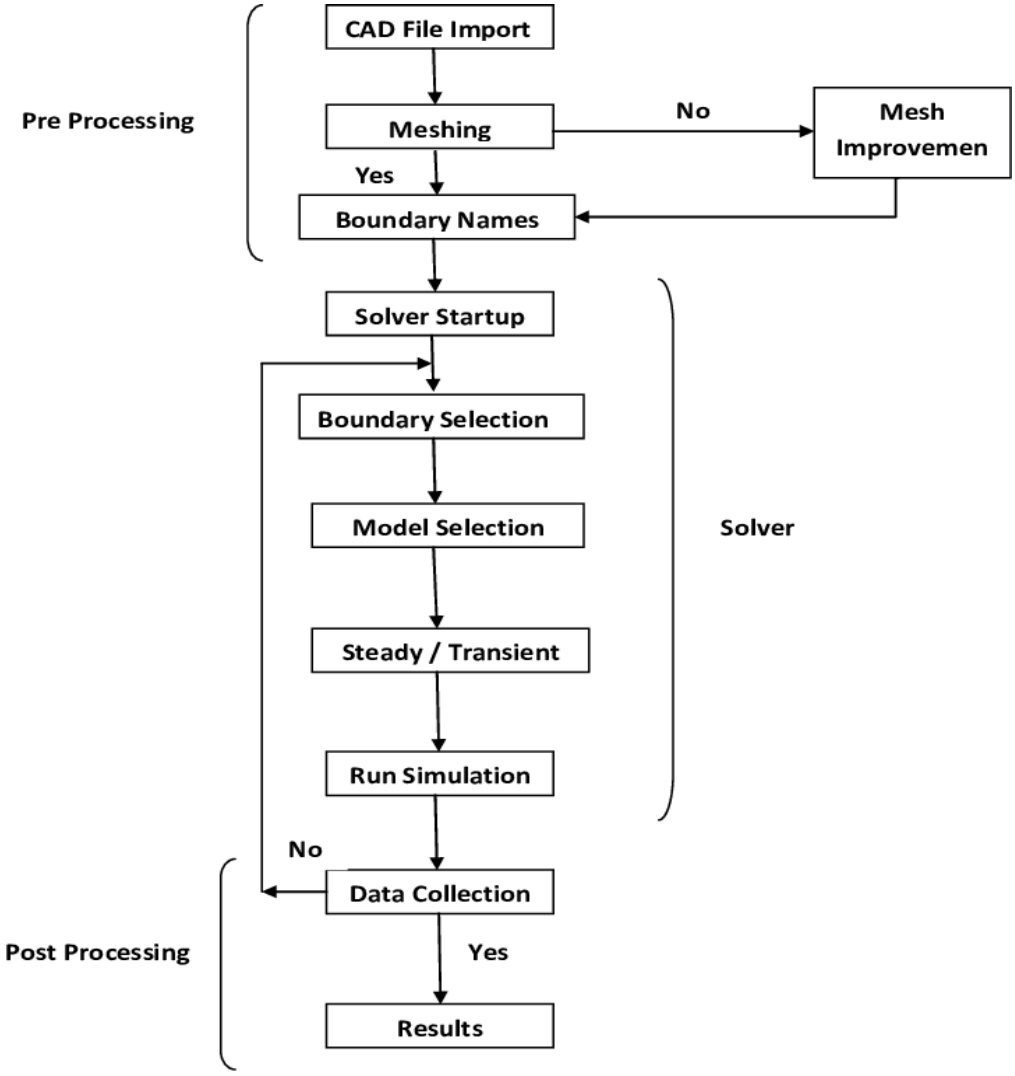

Figure 4. Flow chart of simulation

3. Results and discussion

3.1 Effect of heat exchanger tube diameter on the refrigeration cycle

The diameter of the heat exchanger for the manufactured tubes has a significant impact on the refrigeration value of the gas coming from the condenser, which has relatively high temperatures. The results obtained with regard to changing the diameter of the inner tube indicate an increase in the cycle enthalpy at point 3. As shown in Table 3, the composition of the refrigeration cycle is observed by the axes represented as temperatures and the entropy of the cycle through the data mentioned in the numerical work.

Table 3: Results obtained from the EES program without heat exchanger

Point	h [kJ/M]	P [bar]	s [J/K]	T [C]	X	V
1	248.3	678.3	1.181	−5.075	-	0.0101
2	419.8	678.3	1.82	−5	1	0.03852
3	462.9	1889	1.867	58.4	-	0.01636
4	248.3	1889	1.164	30	0	0.000967

Figure 5 shows the thermal effect in the heat exchanger and the method of transferring thermal energy according to the diameter of the tubes in the heat exchangers. During the heat exchange process for the hot outlet, the temperature value is greater at the tube diameter of 6 mm, where the outlet temperature was 23.577 °C. With a diameter of 4 mm, the temperature returns of the outlet reached 22.056 °C. Thus, the cooling coefficient of the heat exchanger is better when the tube diameter is 4 mm. To ensure the accuracy of the readings, the COP value is obtained through the EES program. In this case, the value reached 5.044 at a diameter of 4 mm, and at a diameter of 6 mm, it reached 4.864. This finding further confirms that the heat exchanger is better at 4 mm diameter at other diameters.

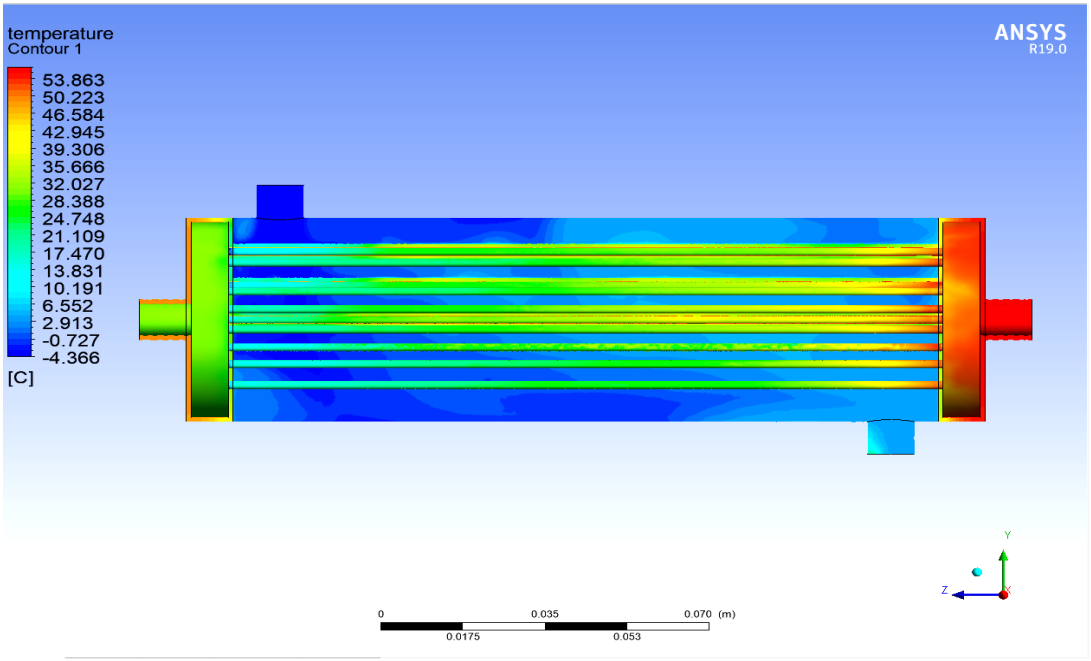

(a)

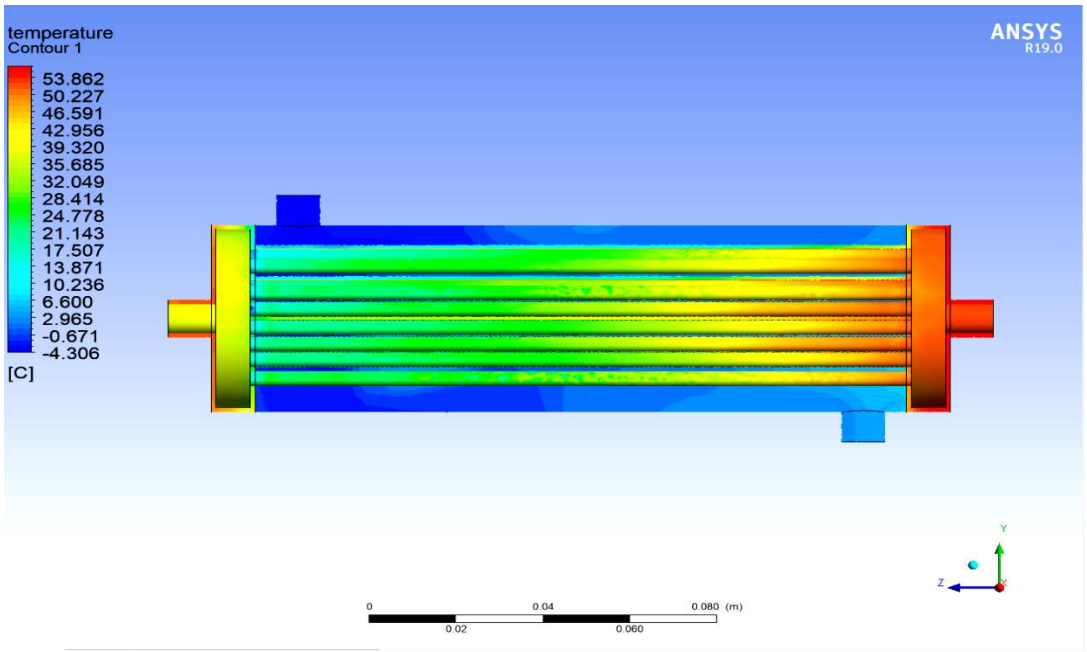

(b)

Figure 5. Temperature contour of heat exchanger (shell and tube) at pipe diameter (a) 4 mm and (b) 6 mm.

This finding can be confirmed by the COP value, which increases the coefficient of the cooling system. This condition is evident in Figure 5, as the shape of the cycle varies according to the diameter of the pipes, and point 4 increased significantly with the value of temperature and entropy. The finding at 4 mm was better than at 6 mm pipe diameter, as shown in Tables 4 and 5.

Table 4: Results obtained from the EES program when the tube diameter is 4 mm, the number of tubes is 17 and the length of the heat exchanger is 150 mm.

point	h [kJ/M]	P [bar]	s [J/K]	T [C]	X	V
1	234.8	678.3	1.131	−5.081	-	0.007877
2	419.8	678.3	1.82	−5	1	0.03852
3	422.8	932.5	1.801	4.975	1	0.0279
4	456.5	1889	1.847	52.89	-	0.01579
5	248.3	1889	1.164	30	0	0.000967
6	234.8	1531	1.12	22.06	0	0.000931

Table 5: Results obtained from the EES program when the tube diameter is 6 mm, the number of tubes is 17 and the length of the heat exchanger is 150 mm.

point	h [kJ/M]	P [bar]	s [J/K]	T [C]	X	V
1	237.4	678.3	1.14	−5.08	-	0.008296
2	419.8	678.3	1.82	−5	1	0.03852
3	422.5	896.4	1.803	3.697	1	0.02906
4	457.3	1889	1.85	53.6	-	0.01587
5	248.3	1889	1.164	30	0	0.000967
6	237.4	1595	1.129	23.58	0	0.000938

The indicate that the enthalpy value at point 3, represented by the outlet of the cold heat exchanger from the evaporator, is higher at 422.8 KJ/M when the tube diameter is 4 mm than when the tube diameter is 6 mm.

3.2 Effect of heat exchanger tube length on the refrigeration cycle

The increase in the length of the heat exchanger greatly affects the value of the exit temperatures and the temperature difference. Figure 6 shows the effect of the length of the heat exchanger on the temperatures. Thus, the significant reduction in temperatures increases the coefficient in the refrigeration cycle, as shown in Figure 6.

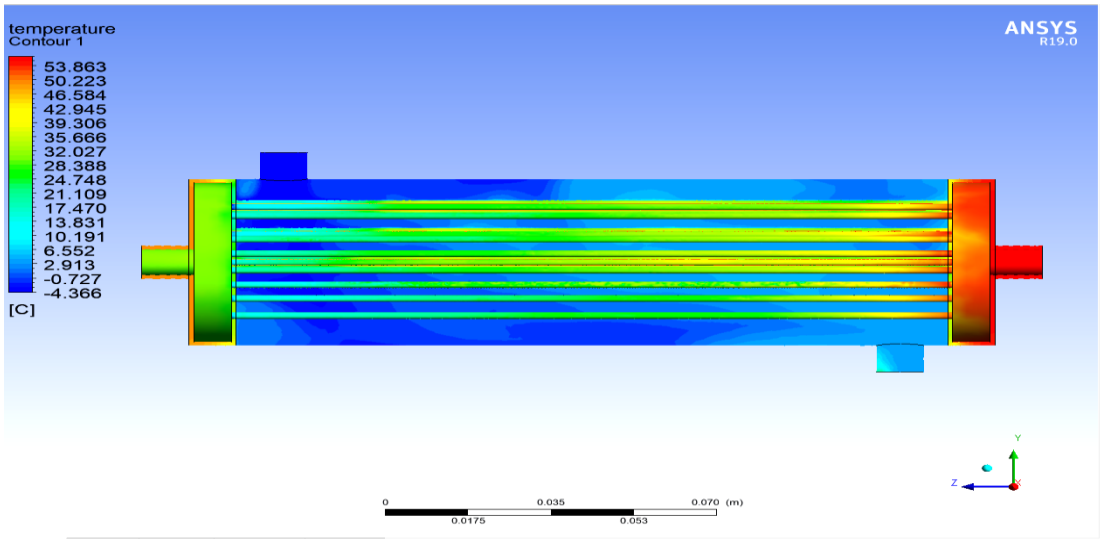

(a)

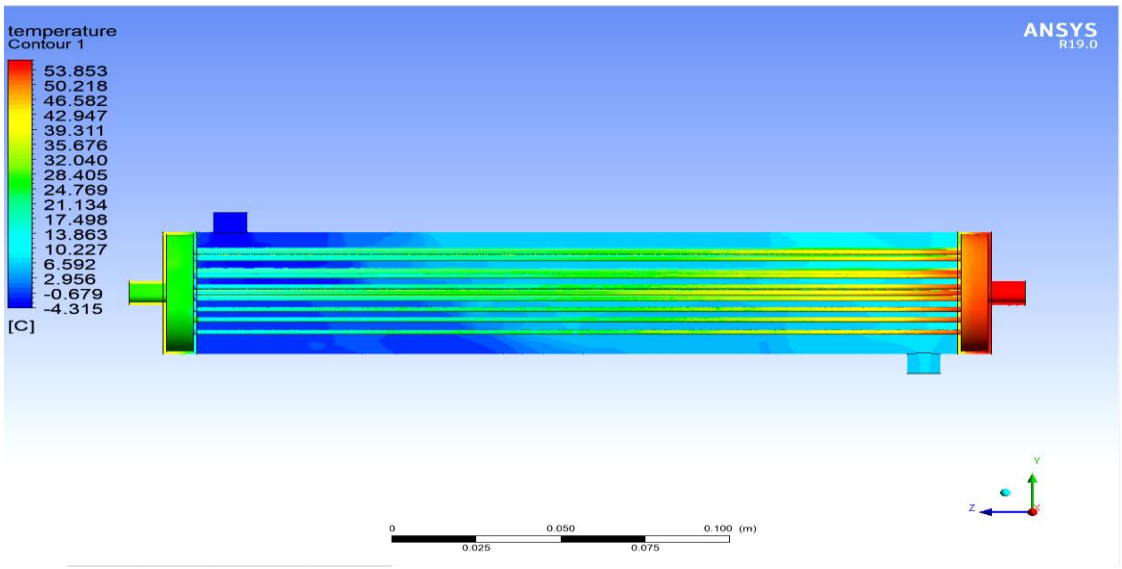

(b)

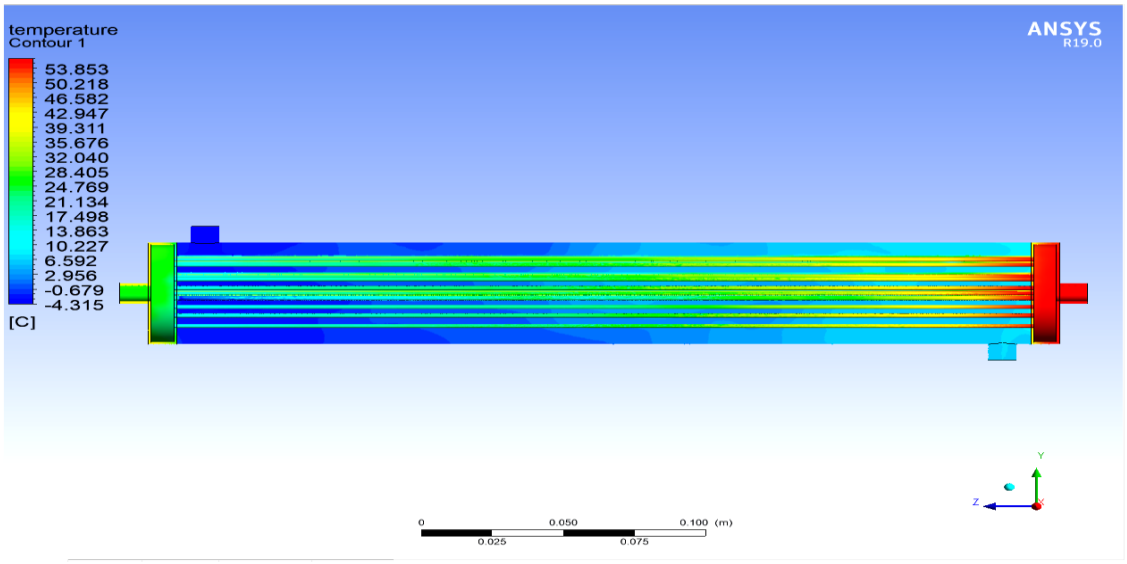

(c)

Figure 6. Temperature contour of heat exchanger (shell and tube) at pipe lengths of (a) 150, (b) 225 and (c) 300 mm.

The figure shows the significant decrease in the exit temperatures with the increase in the length of the heat exchanger. The exit temperature of the heat exchanger on the hot side represented by the condenser reached 22.056 °C for a length of 150 mm with a diameter of 4 mm. The temperature reached 15.73 °C when the length was 225 mm, and it reached 13.847 °C when the length was 300 mm. The cooling coefficient in the heat exchanger increases when the length of the heat exchanger is 300 mm compared with the other lengths.

As shown in Tables 6, 7 and 8, and through the relationship between temperature and entropy, the difference in the cycle temperature values is observed. In addition, as the value of point 4 decreases with the increase in the temperature difference, i.e., the increase in the length of the heat exchanger. Thus, the best condition is reached when the length of the heat exchanger is 300 mm.

Table 6: Results obtained from the EES program when the tube diameter is 4 mm, the number of tubes is 17 and the length of the heat exchanger is 150 mm.

point	h [kJ/M]	P [bar]	s [J/K]	T [C]	X	V
1	234.8	678.3	1.131	−5.081	-	0.007877
2	419.8	678.3	1.82	−5	1	0.03852
3	422.8	932.5	1.801	4.975	1	0.0279
4	456.5	1889	1.847	52.89	-	0.01579
5	248.3	1889	1.164	30	0	0.000967
6	234.8	1531	1.12	22.06	0	0.000931

Table 7: Results obtained from the EES program when the tube diameter is 4 mm, the number of tubes is 17 and the length of the heat exchanger is 225 mm.

point	h [KJ/M]	P [bar]	s [J/K]	T [C]	X	V
1	224.5	678.3	1.092	−5.086	-	0.00617
2	419.8	678.3	1.82	−5	1	0.03852
3	423.2	979.4	1.798	6.586	1	0.02653
4	455.4	1889	1.844	52	-	0.0157
1	248.3	1889	1.164	30	0	0.000967
6	224.5	1285	1.086	15.73	0	0.000906

Table 8: Results obtained from the EES program when the tube diameter is 4 mm, the number of tubes is 17 and the length of the heat exchanger is 300 mm.

point	h [kJ/M]	P [bar]	s [J/K]	T [C]	X	V
1	221.5	678.3	1.081	−5.087		0.005671
2	419.8	678.3	1.82	−5	1	0.03852
3	423.2	978.4	1.798	6.552	1	0.02656
4	455.4	1889	1.844	52.01		0.0157
5	248.3	1889	1.164	30	0	0.000967
6	221.5	1217	1.076	13.85	0	0.0009

Tables that present the results obtained through the EES program show that the heat exchanger with a length of 300 mm is preferred over others. This preference is discerned through the enthalpy values specific points. At point 3, corresponding to the evaporator exit, the enthalpy value is 423.2 kJ/M. By contrast, at point 6, representing the exit, the enthalpy decreases to 221.5 kJ/M.

3.3 Effect of heat exchanger length and tube diameter on COP

The exit temperature of the heat exchangers decreases as the length of the heat exchangers increases. As a result, the COP of the cooling system increases. Figure 6 shows that the value of the hot temperatures decreases dramatically with an increase in the length of the heat exchanger, and an opposite behaviour is observed on the cold side. In addition, the best COP reached is 5.566 when the length of the heat exchanger is 300 mm and the diameter of the tubes is 4 mm.

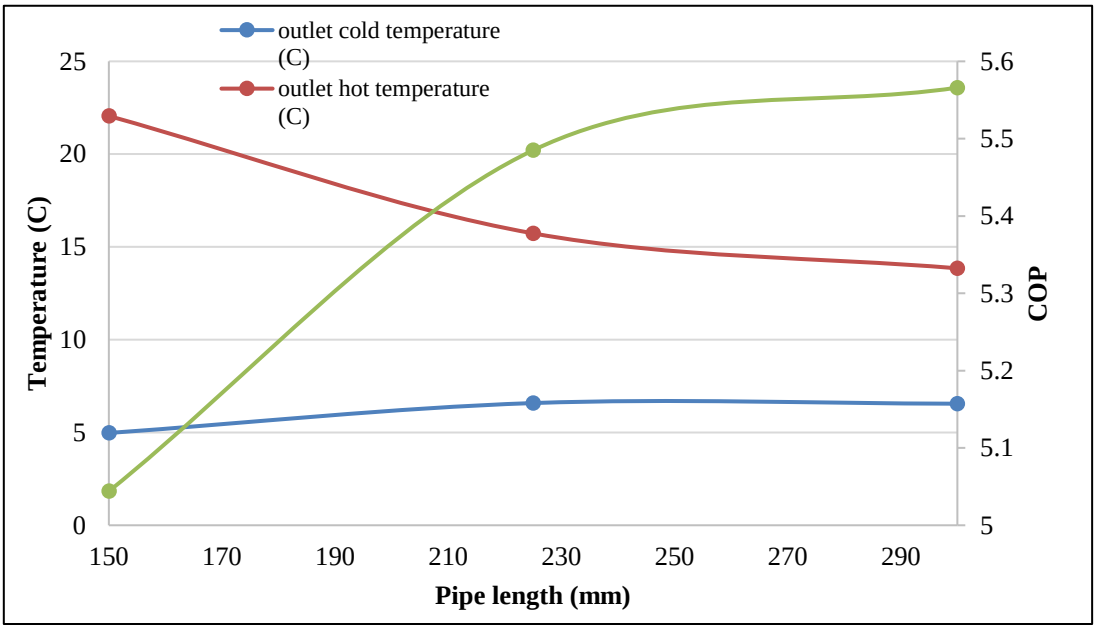

Figure 7. COP and temperature with pipe length at 4 mm diameter pipe

Figure 8 shows that at pipe diameter of 6 mm, the same features are observed, namely, the increase in the length of the heat exchanger decreases the value of the exit temperatures for the hot side. The COP value at the diameter of 6 mm reached 5.24 at the length of the heat exchanger of 300 mm, which is lower than at the diameter of 4 mm.

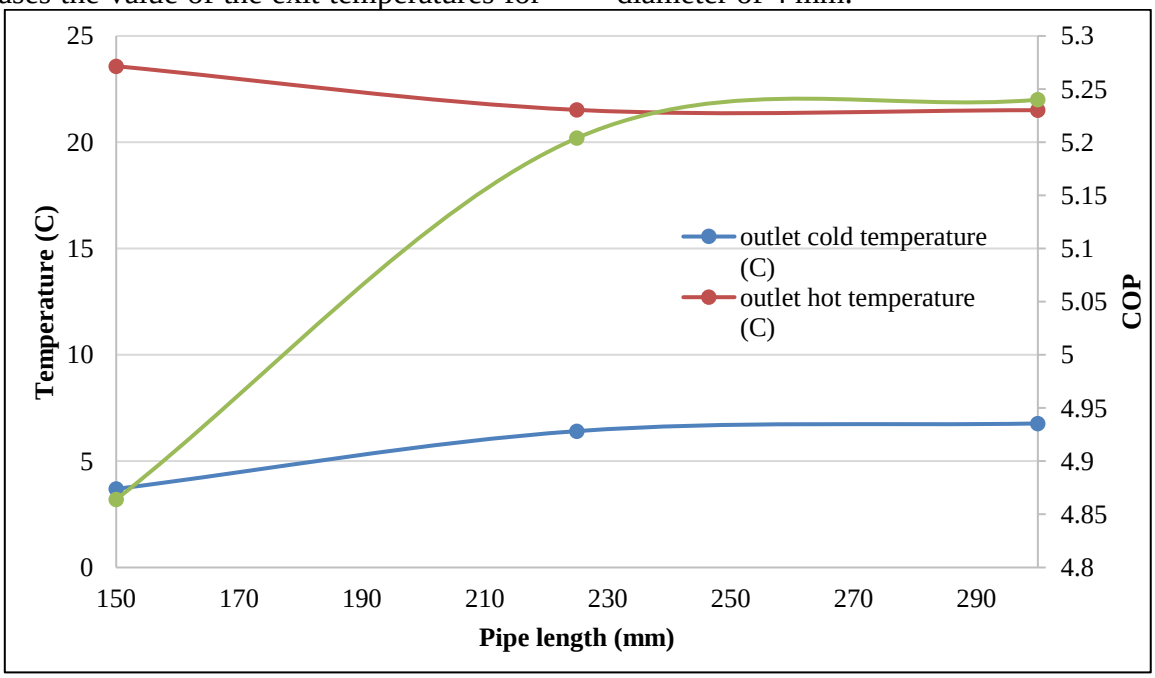

Figure 8. COP and temperature with pipe length at 6 mm dimeter pipe

Table 9 presents the exit temperatures of the heat exchanger and the performance coefficient according to the different variables used in the design of the heat exchanger. Determining the optimal design preference for heat exchanger is possible by calculating the highest cycle performance coefficient.

Table 9: Exit temperatures of the heat exchanger and the performance coefficient according to the variables used in the design of the heat exchanger.

Tube dimeter (mm)	Number of tubes	Length pipe (mm)	Outlet cold temperature (°C)	Outlet hot temperature (°C)	COP
4	9	150	3.98	33.08	4.452
4	9	225	5.26	23.59	5.001
4	9	300	5.24	20.77	5.127
4	13	150	4.47	28.67	4.699
4	13	225	5.92	20.44	5.206
4	13	300	5.89	18.00	5.314
4	17	150	4.97	22.05	5.044
4	17	225	6.58	15.73	5.485
4	17	300	6.55	13.84	5.566
6	17	150	3.69	23.57	4.864
6	17	225	6.41	21.52	5.204
6	17	300	6.77	21.50	5.24

4. Conclusions

The results obtained from the simulation programs are summarised in detail, as follows:

1. The measurement of the intensity exchanger for the produced tubes fundamentally affects the refrigeration worth of the gas from the condenser, which has moderately high temperatures. The cycle state fluctuates with the breadth of lines, and point 4 expands remarkably in the temperature and entropy values. The pipe with a diameter of 4 mm provided better results than that with a 6 mm diameter. This finding can be confirmed by the COP of approximately 5.566, leading to the productivity of the cooling framework.
2. The length of the heat exchanger remarkably influences the outlet temperatures and the temperature distinction. For a length of 225 mm, the temperature reached 15.73 °C and for 300 mm it decreased to 13.847 °C. The critical decrease in temperatures expands the productivity in the refrigeration cycle. High productivity of cooling in the intensity exchanger is obtained when the length is 300 mm contrary to that with different lengths.
3. The best COP is 5.566 when the length of the intensity exchanger is 300 mm and the width of the cylinders is 4 mm. The value of hot temperatures diminishes emphatically with an expansion in the length, exhibiting an opposite trend for the cold side. Concerning the line measurement of 6 mm, similar characteristics are observed, namely, an increase in size diminishes the value of the outlet temperatures for the hot side.

References

[1] Sumeru, T.P. Pramudantoro, F.N. Ani, H. Nasution, Enhancing Air Conditioning Performance Using TiO_2 Nanoparticles in Compressor Lubricant, Adv. Mater. Res. 1125 (2015) 556–560. https://doi.org/10.4028/www.scientific.net/amr.1125.556.

[2] R.I. Tritjahjono, K. Sumeru, A. Setyawan, M.F. Sukri, Evaluation of Subcooling with liquid-suction heat exchanger on the performance of air conditioning system using R22/R410A/R290/R32 as refrigerants, J. Adv. Res. Fluid Mech. Therm. Sci. 55 (2019) 1–11.

[3] K. Sumeru, C. Sunardi, M.F. Sukri, Effect of

compressor discharge cooling using condensate on performance of residential air conditioning system, AIP Conf. Proc. 2001 (2018). https://doi.org/10.1063/1.5049962.

[4] S. Choi, U. Han, H. Cho, H. Lee, Review: Recent advances in household refrigerator cycle technologies, Appl. Therm. Eng. 132 (2018) 560–574. https://doi.org/10.1016/j.applthermaleng.2017.12.133.

[5] V. Pérez-García, J.M. Belman-Flores, J.L. Rodríguez-Muñoz, V.H. Rangel-Hernández, A. Gallegos-Muñoz, Second law analysis of a mobile air conditioning system with internal heat exchanger using low GWP refrigerants, Entropy. 19 (2017). https://doi.org/10.3390/e19040175.

[6] S. Qian, J. Yu, G. Yan, A review of regenerative heat exchange methods for various cooling technologies, Renew. Sustain. Energy Rev. 69 (2017) 535–550. https://doi.org/10.1016/j.rser.2016.11.180.

[7] J.F. Ituna-Yudonago, J.M. Belman-Flores, F. Elizalde-Blancas, O. García-Valladares, Numerical investigation of CO2 behavior in the internal heat exchanger under variable boundary conditions of the transcritical refrigeration system, Appl. Therm. Eng. 115 (2017) 1063–1078. https://doi.org/10.1016/j.applthermaleng.2017.01.042.

[8] A. Mota-Babiloni, J. Navarro-Esbrí, J.M. Mendoza-Miranda, B. Peris, Experimental evaluation of system modifications to increase R1234ze(E) cooling capacity, Appl. Therm. Eng. 111 (2017) 786–792. https://doi.org/10.1016/j.applthermaleng.2016.09.175.

[9] J.M. Belman-Flores, A.P. Rodríguez-Muñoz, C.G. Pérez-Reguera, A. Mota-Babiloni, Étude expérimentale sur le remplacement immédiat du R134A par du R1234yf dans un réfrigérateur domestique, Int. J. Refrig. 81 (2017) 1–11. https://doi.org/10.1016/j.ijrefrig.2017.05.003.

[10] Prayudi, R. Nurhasanah, R.A. Diantari, The effect the effectiveness of the liquid suction heat exchanger to performance of cold storage with refrigerant R22, R404A and R290/R600a, AIP Conf. Proc. 1788 (2017). https://doi.org/10.1063/1.4968320.

[11] H. Cho, C. Park, Experimental investigation of performance and exergy analysis of automotive air conditioning systems using refrigerant R1234yf at various compressor speeds, Appl. Therm. Eng. 101 (2016) 30–37. https://doi.org/10.1016/j.applthermaleng.2016.01.153.

[12] A. Mota-Babiloni, J. Navarro-Esbrí, F. Molés, Á.B. Cervera, B. Peris, G. Verdú, A review of refrigerant R1234ze(E) recent investigations, Appl. Therm. Eng. 95 (2016) 211–222. https://doi.org/10.1016/j.applthermaleng.2015.09.055.

[13] G. Pottker, P. Hrnjak, Effect of the condenser subcooling on the performance of vapor compression systems, Int. J. Refrig. 50 (2015) 156–164. https://doi.org/10.1016/j.ijrefrig.2014.11.003.

[14] M.F. Sukri, M.N. Musa, M.Y. Senawi, H. Nasution, Achieving a better energy-efficient automotive air-conditioning system: a review of potential technologies and strategies for vapor compression refrigeration cycle, Energy Effic. 8 (2015) 1201–1229. https://doi.org/10.1007/s12053-015-9389-4.

[15] M. Ramadan, M.G. El Rab, M. Khaled, Parametric analysis of air-water heat recovery concept applied to HVAC systems: Effect of mass flow rates, Case Stud. Therm. Eng. 6 (2015) 61–68. https://doi.org/10.1016/j.csite.2015.06.001.

[16] Z. Qi, Performance improvement potentials of R1234yf mobile air conditioning system, Int. J. Refrig. 58 (2015) 35–40. https://doi.org/10.1016/j.ijrefrig.2015.03.019.

[17] M. Xing, R. Wang, J. Yu, Application of fullerene C60 nano-oil for performance enhancement of domestic refrigerator compressors, Int. J. Refrig. 40 (2014) 398–403. https://doi.org/10.1016/j.ijrefrig.2013.12.004.

[18] K. Sumeru, S. Sulaimon, H. Nasution, F.N. Ani, Numerical and experimental study of an ejector as an expansion device in split-type air conditioner for energy savings, Energy Build. 79 (2014) 98–105.https://doi.org/10.1016/j.enbuild.2014.04.043.

[19] A. Mota-Babiloni, J. Navarro-Esbrí, Á. Barragán, F. Molés, B. Peris, Drop-in energy performance evaluation of R1234yf and R1234ze(E) in a vapor compression system as R134a replacements, Appl. Therm. Eng. 71 (2014) 259–265. https://doi.org/10.1016/j.applthermaleng.2014.06.056.

[20] K. Sumeru, H. Nasution, F.N. Ani, Numerical study of ejector as an expansion device in split-type air conditioner, Appl. Mech. Mater. 388 (2013) 101–105. https://doi.org/10.4028/www.scientific.net/AMM.388.101.

[21] Krishna, Akshay Bharadwaj, et al. “Technoeconomic Optimization of Superalloy Supercritical CO2 Microtube Shell-And-Tube-Heat Exchangers.” Applied Thermal Engineering, vol. 220, Feb. 2023, p. 119578, doi:https://doi.org/10.1016/j.applthermaleng.2022.119578.

[22] Khan, Abdullah, et al. “Numerical and Experimental Analysis of Shell and Tube Heat Exchanger with

Round and Hexagonal Tubes." Energies, vol. 16, no. 2, Jan. 2023, p. 880, doi:https://doi.org/10.3390/en16020880.

[23] "Ansys | Engineering Simulation Software." www.ansys.com, ansys.com.